Current Research in Food Science 9 (2024) 100883

Contents lists available at ScienceDirect

Current Research in Food Science

journal homepage: www.sciencedirect.com/journal/current-research-in-food-science

Microbial community assembly patterns at the species level in different parts of the medium temperature Daqu during fermentation

Zhang Wen [a,b,1], Pei-Jie Han [a,*,1], Da-Yong Han [a], Liang Song [a], Yu-Hua Wei [a,b], Hai-Yan Zhu [a,b], Jie Chen [c], Zheng-Xiang Guo [c], Feng-Yan Bai [a,b,**]

[a] State Key Laboratory of Mycology, Institute of Microbiology, Chinese Academy of Sciences, Beijing, 100101, PR China
[b] College of Life Science, University of Chinese Academy of Sciences, Beijing, 100049, PR China
[c] Yibin Nanxi Liquor Co., Ltd., Yibin, 644000, PR China

ARTICLE INFO

Handling Editor: Dr. Siyun Wang

Keywords:
Medium temperature Daqu
Microbial community assembly
Endogenous driving factors
Co-occurrence network
PacBio SMRT sequencing

ABSTRACT

Medium-temperature Daqu (MT-Daqu) serves as a crucial saccharifying and fermentation agent in the production of strong-flavor Baijiu. Due to the spatial heterogeneity of solid fermentation, significant differences occurred in the fermentation state and appearance features in different parts of Daqu during fermentation. Currently, the understanding of the underlying mechanism behind this phenomenon remains limited. Here, we analyzed the microbial succession and assembly models and driving factors in different parts of MT-Daqu at the species level based on the PacBio single-molecule real-time sequencing technology. The results showed significantly different bacterial and fungal community compositions, successions, and interaction patterns in different parts of MT-Daqu. The bacterial community composition and succession model in the middle layer were similar to those in the core layer, whereas the fungal community composition and succession model in the surface layer were similar to those in the middle layer. The co-occurrence network analysis showed that microbial interaction is stronger in the middle and core layers than in the surface layer. Analyses based on both niche theory and neutral theory models indicated that deterministic processes predominantly governed the microbial community assembly and these processes played an increasingly important role from the surface to the core layer. Random forest analysis revealed that temperature was the primary endogenous factor driving the bacterial and fungal community assembly. The results of this study contribute to a better understanding of the microbial community in MT-Daqu and are helpful for the quality control of MT-Daqu fermentation.

1. Introduction

Chinese Baijiu is unparalleled in the world of spirits and distinguished by its unique taste and flavor, resulting from its unique solid-state fermentation and distillation technology (Sakandar et al., 2020). The production process of Baijiu primarily involves two separate steps: Daqu making and alcoholic fermentation. Daqu is usually produced by spontaneous fermentation of wheat and used as the starter to initiate the alcoholic fermentation step. Wheat is firstly grounded, moistened and shaped into bricks, which are then stacked in fermentation rooms and covered with straw mats for spontaneous fermentation for usually 20~40 days to enrich various bacteria and fungi, as well as various enzymes and flavor compounds. Fermented Daqu bricks are stored in room temperature for several months for maturation and the mature Daqu bricks are finally powdered and mixed with steamed and gelatinized sorghum to start alcoholic fermentation (Han et al., 2023). Daqu is mainly classified into three categories based on the maximum temperature achieved during the fermentation process: high-temperature Daqu (HT-Daqu, 60–70 °C), medium-temperature Daqu (MT-Daqu, 50–60 °C), and low-temperature Daqu (LT-Daqu, 40–50 °C), which are used for the fermentation of Jiangxiangxing (sauce-flavor), Nongxiangxing (strong-flavor), and Qingxiangxing (light-flavor) Baijiu, respectively (Han et al., 2024; Jin et al., 2017; Sakandar et al., 2020). Nongxiangxing Baijiu fermented using MT-Daqu and primarily produced in Sichuan and Jiangsu provinces of China, dominates the Chinese Baijiu market and shares roughly 70% of the total Chinese Baijiu market in recent years

* Corresponding author.
** Corresponding author. State Key Laboratory of Mycology, Institute of Microbiology, Chinese Academy of Sciences, Beijing, 100101, PR China.
E-mail addresses: hanpj@im.ac.cn (P.-J. Han), baify@im.ac.cn (F.-Y. Bai).
[1] These authors contributed equally to this work.

https://doi.org/10.1016/j.crfs.2024.100883
Received 14 August 2024; Received in revised form 27 September 2024; Accepted 10 October 2024
Available online 11 October 2024

(Tang et al., 2023; Yang et al., 2024).

Due to the traditional spontaneous fermentation process of Daqu in an open environment, the microbes enriched in Daqu bricks mainly originate from raw materials, tools and the surrounding environment (Pan et al., 2023). The microbial community of Daqu significantly affects the quality of Daqu and consequently the yield and flavor of the final Baijiu product (Han et al., 2023). Previous studies showed that various abiotic factors, including environmental variables such as temperature, humidity, CO_2 and O_2 levels, as well as endogenous variables including core temperature, moisture, and acidity of Daqu (Li et al., 2016; Ma et al., 2022), exert direct or indirect effects on the microbial community composition and succession during the fermentation process of Daqu. Understanding the ecological process that govern the assembly of the microbial community in Daqu is certainly valuable for a more effective control of the fermentation process of Daqu to enhance the quality and stability of the product.

Ecological niche theory and neutrality theory are usually used to address deterministic and stochastic processes, respectively, in explaining microbial community assembly (Nemergut et al., 2013). The niche theory claims that deterministic processes primarily regulate microbial communities through biotic factors (e.g., competition, mutualism, and predation) and abiotic factors (e.g., pH, temperature, and O_2), whereas the neutral theory emphasize that stochastic processes (e.g., birth, death, mutation, limited dispersal, and immigration) play a main role in shaping microbial community assembly (Yang et al., 2023). The ecological methodologies and theories have been used to analyze and explain the microbial assembly in Daqu primarily based on the sequence data obtained from the next-generation sequencing (NGS) technology (Shi et al., 2024; Tang et al., 2023). However, only partial 16S rRNA gene sequences of bacteria and partial ITS region sequences of fungi were obtained in previous studies, and thus the microbial operational taxonomic units (OTUs) or amplicon sequence variants (ASVs) obtained were identified only to the genus level, resulting in a limited resolution of the microbial diversity and assembly pattern in Daqu.

In recent years, the PacBio small-molecule real-time (SMRT) sequencing technology (Karst et al., 2021) has been employed to obtain the full-length 16S and ITS sequences, resulting in an improved understanding of the microbial diversity in Daqu at the species level (Han et al., 2023; Yang et al., 2022; Zhang et al., 2022b). However, these studies mainly used thoroughly mixed samples of Daqu bricks. Due to the solid-state fermentation nature of Daqu, the physicochemical changes in different parts of a Daqu brick are quite different, resulting in the differences in microbial diversity and community assembly from the surface to the core of Daqu bricks (Tang et al., 2023). The microbial assembly patterns and the factors shaping the microbial assembly in different parts of a Daqu brick remain to be fully revealed.

In this study, we analyze the diversity of microbes in the surface, middle and core layers of MT-Daqu bricks in different stages of the fermentation process based on the full-length 16S and ITS rDNA amplicon sequences obtained using the PacBio SMRT sequencing technology. Simultaneously, we monitored the changes of physiochemical characteristics in different layers of Daqu during the fermentation process. We aimed to address (1) the temporal and spatial variations of the microbial community of MT-Daqu during the fermentation process, (2) whether the microbial community assembly patterns are governed by deterministic or stochastic processes, and (3) the endogenous factors that significantly influence the microbial diversity and community assembly.

2. Materials and methods

2.1. Sample collection

The MT-Daqu sampled was produced in May 2022 in a Baijiu distillery in Yibin, Sichuan province, China. The whole fermentation period of Daqu was 25 days. Daqu bricks with different fermentation times (day 0, 1, 2, 4, 7, 10, 15, 20 and 25) were randomly collected from three different locations (near the door, the center, and near the window) in the fermentation room (Fig. 1a). A total of 27 Daqu bricks consisted of nine groups (with three samples each) with different fermentation times were collected. A Daqu brick was divided into three parts (Fig. 1b): the surface layer (S-layer, 0–1 cm from the surface), the middle layer (M-layer, 1–3 cm from the surface) and the core layer (C-layer). Each part was crushed separately and approximately 500 g Daqu powder from each part was collected in a sterile plastic bag. Finally, a total of 81 samples, including 27 S-, M-, and C-layer samples each were collected. Each Daqu sample was then divided into two parts: one for physiochemical parameter measurement (stored at 4 °C) and the other for genomic DNA extraction (stored at −80 °C).

2.2. Endogenous factors parameter determination

Numerous physicochemical parameters in Daqu spontaneously arise during fermentation, thus they are designated as endogenous factors. The temperature in different parts of Daqu during fermentation was recorded by electronic temperature sensors (Jinming, Tianjin, China) embedded in Daqu bricks. Moisture, pH, total acidity, and enzymatic properties (including saccharifying, liquefying, and acidic protease activities) were assessed following the standard protocols outlined in the *General Methods of Analysis for Daqu of China* (QB/T4257-2011).

The contents of sugars, alcohols, and organic acids in Daqu samples were measured using the methods described in a previous study (Wu et al., 2023). Free amino acids were determined using HPLC equipped with an AJS-02 amino acid analysis column (C18, 4.6 × 150 mm, 3 μm, Shimadzu) and a photodiode array detector. The mobile phase consisted of solvent A (4.5% $Na_2HPO_4{\cdot}12H_2O$, 4.75% $Na_2B_4O_7{\cdot}10H_2O$, pH 8.2) and solvent B (4.5% methanol, 4.5% acetonitrile, 10% water). Elution was carried out with a binary gradient. The flow rate and injection volume were set at 2.0 mL/min and 2 μL, respectively. The column oven temperature was maintained at 50 °C, and the photo diode array (PDA) detector was set at 262 nm and 338 nm to monitor the derivatized amino acids.

2.3. High-throughput sequencing and bioinformatic analysis

Genomic DNA from Daqu samples was extracted using the protocol described in (Han et al., 2024). The primer pair 27F (5′-AGA GTT TGA TCC TGG CTC AG-3′) and 1492R (5′-TAC GAC TTA ACC CCA ATC GC-3′) was utilized to amplify the full-length bacterial 16S rRNA gene and the primer pair ITS1F (5′-TAC GAC TTA ACC CCA ATC GC-3′) and ITS4R (5′-TCC TCC GCT TAT TGA TAT GC-3′) was applied to amplify the entire internal transcribed spacer (ITS) region of fungi. The 16S rRNA gene was amplified using the following conditions: denaturation at 98 °C for 2 min; 32 cycles of denaturation at 98 °C for 10 s, annealing at 55 °C for 10 s, and extension at 72 °C for 22 s; and a final extension at 72 °C for 5 min. The ITS amplification procedure was 98 °C for 2 min; 32 cycles of denaturation at 98 °C for 10 s, annealing at 56 °C for 10 s, and extension at 72 °C for 15 s; and a final extension at 72 °C for 5 min. Amplicon purification and quantification were performed as per the methods outlined in Luo et al. (2023). Subsequent sequencing was performed utilizing the PacBio Sequel II instrument, following the standard protocols used in Biomarker Technologies Corporation (Beijing, China).

Raw subreads were converted into high-fidelity reads using CCS 6.0.0 and analyzed with the VSEARCH 2.14 (Rognes et al., 2016) and USEARCH 11 software. Barcodes and primers were removed using the *fastx_truncate* command. Chimeric sequences were identified and eliminated by comparing them to the UNITE CHIME reference dataset using the *uchime_re* command (Nilsson et al., 2015). Non-chimeric sequences were then de-replicated with the *fastx_uniques* command. Subsequently, unique sequences were clustered into amplicon sequence variants (ASVs) at 100% nucleotide sequence similarity using the *unoise3* command, with a minimum cluster size of 10 (Prodan et al., 2020). The

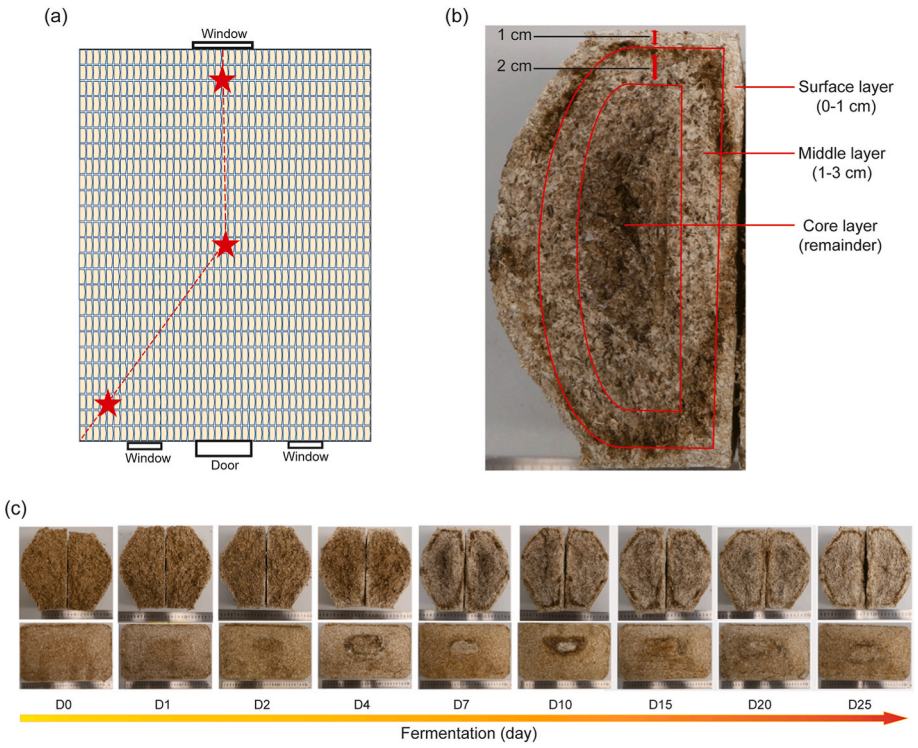

Fig. 1. The sampling strategy and temporal development of MT-Daqu during fermentation. (a) Locations (indicated by red stars) of the Daqu bricks sampled in the fermentation room. Morphological changes of the surface (upper) and cross-section (lower) of Daqu throughout the fermentation process. (b) Sketch of the cross-section of a Daqu brick showing the surface, middle, and core layers sampled. (c) Morphological changes of the surface (upper) and cross-section (lower) of Daqu throughout the fermentation process. (For interpretation of the references to color in this figure legend, the reader is referred to the Web version of this article.)

resulting ASV sequences were blasted against the type strains in the NCBI database, using an identity threshold of more than 97% and alignment coverage threshold of more than 90% to decide the species of the ASVs. The non-microbial sequences were removed. The final ASV table was constructed using the *usearch_global* command with a 97% similarity threshold.

2.4. Statistical analysis

GraphPad Prism 9 was used to visualize the results related to the endogenous factors of Daqu. Data analysis was performed using R software version 4.2.2, unless otherwise stated. The alpha diversity indices (Richness index and Gini-Simpson diversity index) and principal component analysis (PCoA) were conducted using the vegan package (version 2.6–4). Permutational multivariate analysis of variance (PERMANOVA) and analysis of similarity (ANOSIM) were employed to assess the significance of microbial community dissimilarities. Spearman correlation analysis was conducted using the psych and reshape2 packages. Co-occurrence events were determined to be statistically significantly correlated ($|r| > 0.6$, $p < 0.05$) using Spearman's correlation test. The co-occurrence network was then visualized using a combination of the igraph package, WGCNA package, and Gephi 0.9.1 software to create co-occurrence network diagrams (Wu et al., 2023).

We employed a range of models to explore microbial community assembly processes in different parts of Daqu during fermentation. Specifically, we conducted the following analyses: (i) assessment of the fit of the neutral community model (R^2) was executed utilizing the Hmisc package (Mo et al., 2021); (ii) calculation of the modified stochasticity ratio (MST), employing a null-model based statistical framework, was performed using the NST package based on Jaccard distance (Ning et al., 2019); (iii) evaluation of the deviation of each observed metric from the average of the null model (checkerboard score, C-score) was conducted using the EcoSimR package (Mo et al., 2021); and (iv) determination of Levins' niche breadth index was carried out utilizing the *niche. width* function within the spaa package.

Mantel test analysis was conducted using the vegan package to investigate the Pearson's correlation between each endogenous factors and microbial communities in different parts of MT-Daqu. To develop a model correlating the microbial community composition of MT-Daqu with each layer during fermentation, the randomForest package was utilized to assess the relative abundance (RA) of bacterial and fungal taxa at the species level in different parts of MT-Daqu. Random Forest analysis was employed to assess the impact of endogenous factors on the assembly of the microbial community using the rfPermute package. Statistical significance was defined as $p < 0.05$.

3. Results and discussion

3.1. Temporal changes of appearance features and endogenous factors of MT-Daqu during fermentation

The changes of appearance features in different parts of MT-Daqu can directly reflect the fermentation state and process. The appearance features of MT-Daqu changed significantly and differentiated remarkably in different parts of Daqu bricks during the fermentation process (Fig. 1c). The changes may be caused by the differences in microbial growth and the accumulation of metabolites, such as amino acids and reducing sugars, that undergo a Maillard reaction in different parts of MT-Daqu (Shi et al., 2024). Experienced Daqu-making workers rely on the appearance features of MT-Daqu, to judge the fermentation state and regulate the fermentation progress by adjusting fermentation parameters such as temperature, humidity, O_2, and CO_2 levels. The adjustment is usually achieved by ventilation regulation (opening and closing doors and windows) of the fermentation rooms. Therefore, the appearance features of MT-Daqu are crucial for regulating the fermentation process and evaluating the quality of mature MT-Daqu.

Alterations in the appearance characteristics of MT-Daqu typically parallel with the changes in its microbial composition (Ding et al., 2022). In order to examine the microbial community differences in different parts of MT-Daqu and possible driving forces, the endogenous factors (including physicochemical parameters and enzymatic properties) and microbial characteristics of MT-Daqu were traced during fermentation.

According to the temperature changes of the C-layer of Daqu bricks, the fermentation process underwent three stages: the rising period (Phase I, days 0–6, 24–57 °C); the stable period (Phase II, days 6–13, 57–60 °C); and the cooling period (Phase III, days 13–25, 57∼32 °C) (Fig. 2a). The temperature change trend of the other parts of Daqu basically paralleled with the C-layer during the fermentation process. In the initial period of fermentation, the rapid proliferation and metabolic activity of most microbes lead to the generation of bio-heat within MT-Daqu, and consequently to a substantial temperature rise (Xiao et al., 2017). Meanwhile, the straw mats covering the MT-Daqu bricks and the rice husk laying under them prevented heat dissipation, facilitating rapid increase and prolonged stability of the temperature of MT-Daqu during fermentation. Due to the continuous evaporation during fermentation, the moisture content of different parts of MT-Daqu gradually decreased from about 37% to 11.2%, 12.8%, and 16.6% in the S-, M-, and C-layer, respectively, at the end of fermentation (Fig. 2a).

The pH values changed remarkably during fermentation, showing an initial rapid decrease from day 0 to day 4, followed by a rapid increase from day 4 to day 15, and a final stabilization (Fig. 2b). The lowest pH values were 3.64 and 3.77 detected in the C- and M-layer, respectively on day 4, and 4.64 in the S-layer on day 1. The final pH value of the S-layer was 6.5, being notably lower than those of the M- and C-layer (Fig. 2b). Corresponding changes in total acidity were observed in different parts of MT-Daqu (Fig. 2b). Specifically, the contents of lactic acid and acetic acid increased rapidly at first, then decreased gradually

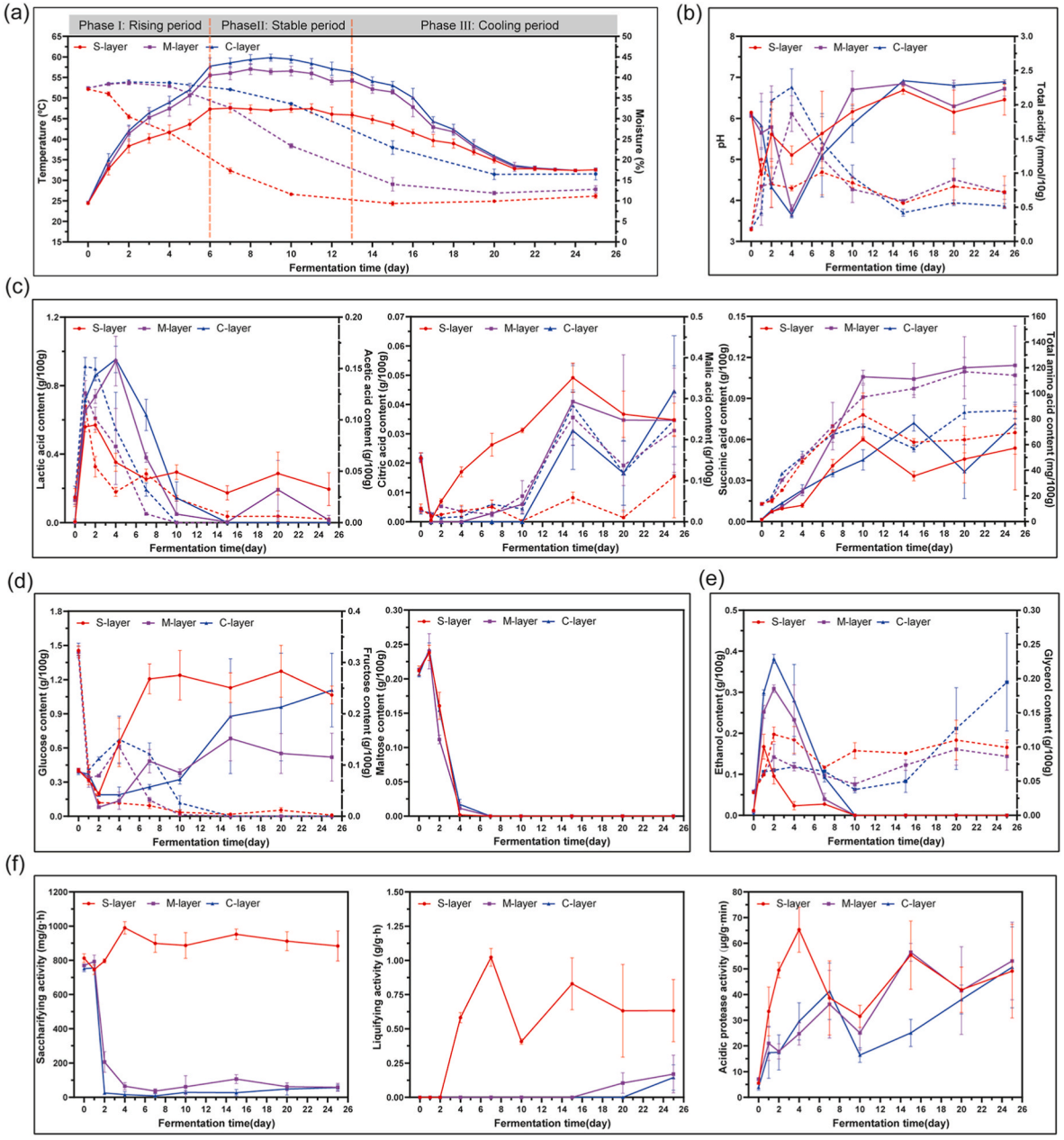

Fig. 2. The dynamics of endogenous physiochemical factors (a–e) and enzyme activities (f) in different parts of MT-Daqu during fermentation. In a-e, the solid polyline and dotted lines correspond to the left and right vertical axes, respectively. Each point represents the average of triplicates ± SE.

with fluctuations during fermentation; while the contents of citric acid, malic acid, succinic acid, and free amino acids showed a gradual increasing trend during fermentation (Fig. 2c).

The glucose content initially decreased rapidly and then increased since day 2 with fluctuations during fermentation (Fig. 2d). The maltose and fructose contents decreased significantly and were completely consumed in the subsequent period (Fig. 2d). The ethanol content increased rapidly in the first two days, then decreased rapidly and became undetectable after 10 days of fermentation (Fig. 2e). The glycerol contents in different parts of MT-Daqu showed a parallel change with ethanol in the first 10 days but then gradually increased, especially in the C-layer (Fig. 2e).

The types and levels of hydrolases in MT-Daqu directly reflect its functionality. The S-layer of Daqu exhibited much higher saccharifying and liquefying activities than the other two parts during fermentation (Fig. 2f). The saccharifying activity (amylase) ranged from 745.17 to 990.30 mg/g·h in the S-layer during the whole fermentation process, and eventually stabilized at about 880 mg/g·h. The initial approximately 750 g/g·h saccharifying activity in the M- and C-layer rapidly decreased to 36.00 mg/g·h in the M-layer and 7.67 mg/g·h in the C-layer on day 7, and eventually reached at 55.7 mg/g·h at the end of fermentation (Fig. 2f). The liquefying activity (glucoamylase) was undetectable in the first two days in the S-layer, but rapidly increased to the peak level of 1.02 g/g·h on day 7 and then gradually decreased to 0.60 g/g·h at the end of fermentation. In the M- and C-layers, the liquefying activity remained undetectable until Day 15 and 20, and reached about 0.12 and 0.60 g/g·h, respectively, at the end of fermentation (Fig. 2f). The variation in saccharifying and liquefying abilities in different parts of MT-Daqu was the primary factor causing differences in reducing sugar content, as these enzymes efficiently convert starch into reducing sugars (Xia et al., 2023).

The acidic protease activity showed a trend of undulant increasing in different parts of MT-Daqu during fermentation, with no significant difference observed at the end of fermentation (Fig. 2f). The acidic protease effectively decomposes proteins, thereby increasing the free amino acid concentration (Fig. 2c). Saccharification, alcoholic fermentation, and flavor generation are three crucial fermentation processes of Nongxiangxing Baijiu using MT-Daqu as the starter. The different parts of MT-Daqu probably play different roles in contributing the microbes and enzymes responsible for the different fermentation processes.

3.2. *Microbial community composition and diversity of MT-Daqu during fermentation*

To investigate the correlation between the endogenous factors and microbial community in MT-Daqu during fermentation, we performed full-length bacterial 16S rRNA gene and fungal ITS region amplicon sequencing from the metagenomes of 81 Daqu samples. After quality control of the reads and chimera and non-microbial sequence removal, a total of 954,394 full-length 16S rRNA gene and 686,553 full-length fungal ITS region sequences were obtained. An average of 11,784 (ranging from 5949 to 23,017) 16S rRNA gene and 8476 (ranging from 1858 to 24,007) ITS sequences per sample were generated. The sequences obtained were clustered into 727 16S and 135 ITS ASVs with 97% similarity. The dilution curve showed that both the bacterial and fungal diversities in the samples approached a plateau, indicating that the sequencing depth was sufficient to cover the majority of the fungal and bacterial taxa in the samples (Fig. S2).

Comparative bacterial and fungal diversity analyses were carried out after normalizing the sequence numbers to ensure equal sequencing depths of all the samples compared. The richness (Richness index) and diversity (Gini-Simpson diversity index) of the microbial communities in different parts of Daqu during fermentation were analyzed. There was no significant difference in the overall bacterial richness in different parts of Daqu (Fig. S3a) during the whole fermentation process, whereas the fungal richness decreased significantly from the S-layer to the C-layer ($p < 0.01$) (Fig. S3d). In the samples with different fermentation times, the richness of bacteria and fungi in different parts initially decreased and then increased during fermentation (Fig. 3a and f). Specifically, the bacterial richness decreased to its lowest level in different parts of Daqu on days 1–2, whereas the fungal richness reached its lowest point on days 7–10.

In terms of species diversity as measured using the Gini-Simpson diversity index, both bacterial and fungal diversity decreased significantly from the S-layer to the C-layer ($p < 0.001$) during the whole fermentation process (Figs. S3b and S3e). The bacterial diversity showed a gradual and consistent increase trend during fermentation in the S-layer, but a remarkable decrease trend in the later stage in the M-layer; while a constant decrease trend during the early and middle stages and a slight increase trend in the later stage in the C-layer (Fig. 3b). For fungi, the diversity in the S-layer showed a slight decrease in the early stage and then a slight increase after day 7; while in the C-layer a dramatic decrease and increase before and after day 7 were observed. In the M-layer, the fungal diversity exhibited a slight downward trend (Fig. 3g).

During the whole fermentation process, the Bray-Curtis heterogeneities of bacterial ($p = 0.003$) and fungal communities ($p = 0.004$) increased gradually from the S-layer to C-layer, with significant differences (Figs. S3c and S3f), which indicated a clear spatial compartmentalization of the bacterial and fungal communities in different parts of Daqu. We observed a clear temporal succession pattern in both bacterial (PERMANOVA: $R^2 = 0.27$, $p = 0.001$; ANOSIM: $R = 0.33$, $p = 0.001$) (Fig. 3c and d) and fungal community structures (PERMANOVA: $R^2 = 0.58$, $p = 0.001$; ANOSIM: $R = 0.45$, $p = 0.001$) (Fig. 3h and i). The variations were explained by the first two axes of PCoA (66.68% for bacteria and 89.55% for fungi) (Fig. 3d and i). The Bray-Curtis heterogeneity of the microbiota in different parts of Daqu exhibited a continuous decline from the beginning to the end of fermentation (Fig. 3e and j), which indicated a clear temporal compartmentalization of the bacterial and fungal communities in different parts of Daqu.

The results indicated that the microbial community succession in different parts displayed spatial variability and temporal heterogeneity during fermentation (Fig. 3c and h, and Fig S4). Specifically, there was a notable succession in the microbial community structure in different parts in the first 7–10 days of fermentation, followed by a relatively stable period. Unlike the S-layer, the bacterial succession patterns in the M-layer and the C-layer were similar, with the main difference occurring after two days of fermentation. On day 0, the bacterial community composition in different parts was largely similar, with LAB being the dominant species, including *Weissella confusa* (30.26%–41.96%), *Leuconostoc citreum* (18.09%–32.89%), and *Weissella cibaria* (11.65%–19.05%) (Fig. 3c). When the bacterial community stabilized in the later stage, the S-layer was predominantly composed of LAB, including *W. confusa* (14.21%–23.96%), *Weissella paramesenteroides* (21.15%–27.37%), and *W. cibaria* (7.18%–22.35%), while the M- and C-layer were dominated by *Bacillus licheniformis* (34.71%–74.10%) (Fig. 3c). In suitable environmental conditions, acid-producing bacteria (LAB) could proliferate rapidly and synthesize a large amount of organic acids (mainly including lactic acid and acetic acid) (Shanqimuge et al., 2015), resulting in an increase in total acidity and a decrease in pH, as shown in Fig. 2b. *B. licheniformis* not only secretes amylolytic and proteolytic enzymes, but also enhances the production of pyrazines and aromatic compounds (Li et al., 2023), all of which contribute to the healthy fermentation and flavor enhancement of Baijiu.

Being different from the bacterial succession pattern, the fungal succession patterns of the S- and M-layer were similar. On day 0, the fungal community compositions in the different parts exhibited a high degree of similarity, with yeasts such as *Pichia kudriavzevii* (47.92%–60.02%), *Wickerhamomyces anomalus* (12.53%–14.15%), and *Pichia fermentans* (5.40%–10.14%) being the predominant species (Fig. 3h). The RA of *P. kudriavzevii* increased in the initial stage, peaking on day 2 in all parts (80.32%–96.67%). With the progress of fermentation, the dominancy of the yeast *P. kudriavzevii* (14.19%–57.25%) was gradually

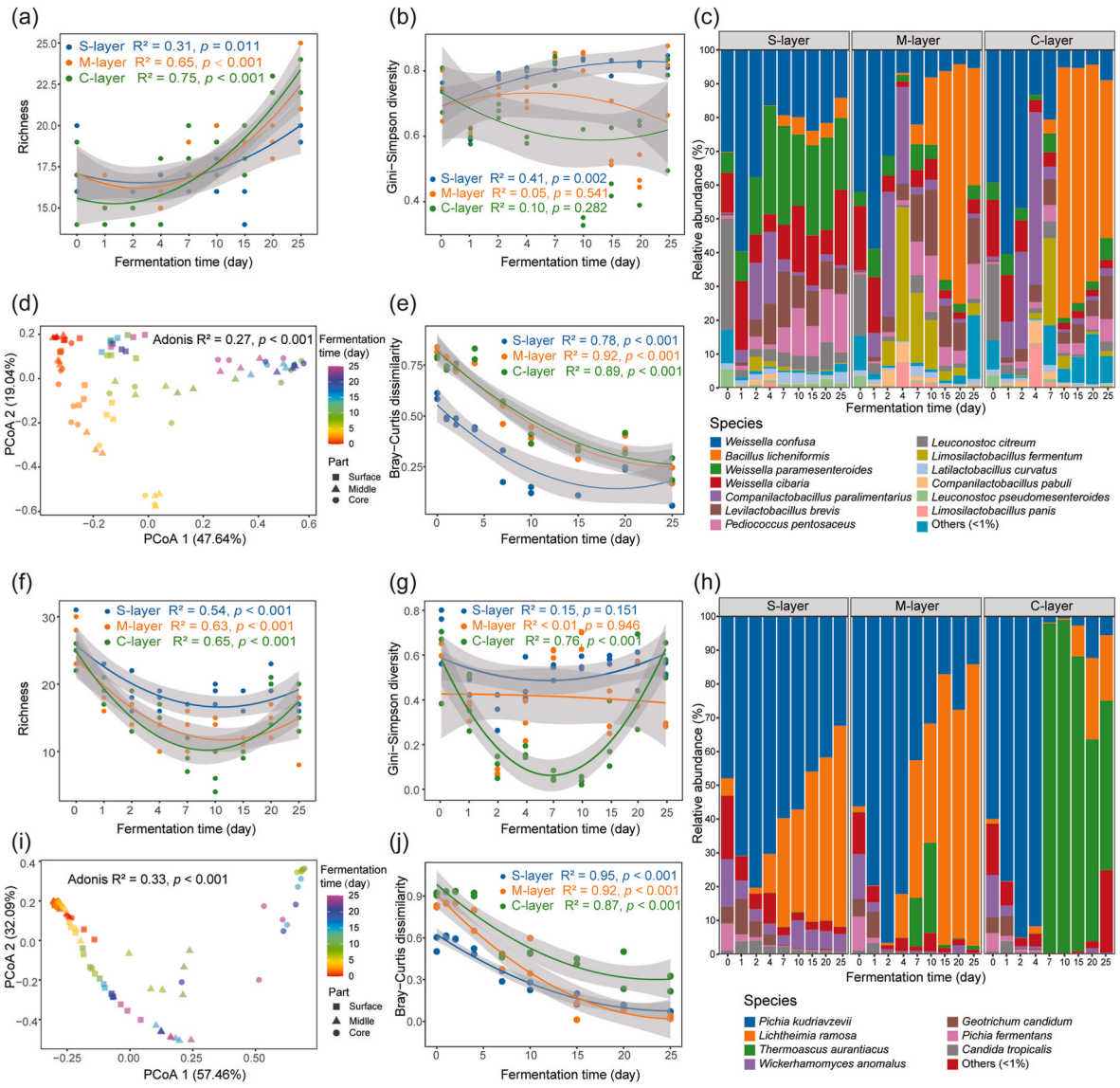

Fig. 3. Temporal dynamics of the diversity, community composition and succession of bacteria (a–e) and fungi (f–j) in different parts of MT-Daqu throughout the fermentation process. Principal coordinate analysis (PCoA) was based on Bray–Curtis distances. Species with a relative abundance less than 1% are classified as 'others'.

replaced by the mould *Lichtheimia ramosa* (30.24%–83.36%) in the S- and M-layer, while replaced by the thermotolerant mould *Thermoascus aurantiacus* (50.19%–98.65%) in the C-layer (Fig. 3h). *P. kudriavzevii* not only serves an ecological role by preserving yeast community diversity and inhibiting fungal overgrowth, but also reduces the presence of certain harmful compounds such as ethyl carbamate in Baijiu fermentation (Du et al., 2022), and has the ability to produce the crucial volatile organic compound 2-phenylethanol (imparting a rose aroma), which is a pivotal Qu-aroma constituent in MT-Daqu (Yang et al., 2024). The high saccharifying and liquifying activities of the S-layer shown in this study are probably mainly contributed by the dominant fungus *L. ramosa* as shown in Fig. 3h. A previous study showed that *L. ramosa* was the predominant fungi converting starch to glucose via glucan 1,4-alpha-glucosidase and glucoamylase in Nongxiangxing Daqu (He et al., 2023), contributing to provide substrates and energy for Daqu and Baijiu fermentation. The thermotolerant fungus *T. aurantiacus* dominating in the C-layer (Fig. 3h) can synthesize a range of thermophilic glycoside hydrolases (beta-glucosidase and beta-xylosidase) (Parry et al., 2000), which probably participate in polysaccharide (cellodextrin) degradation in the core part of MD-Daqu.

Based on the weight values of the microbial species estimated using the random forest learning algorithm, 13 prominent bacterial species and six fungal species were identified as biomarkers that differed significantly between different parts of Daqu in terms of relative abundance (RA) (Figs. S4a and b). Among the biomarker species, the RAs of most LAB (such as *L. pseudomesenteroides*, *W. confusa*, and *W. cibaria*) and fungi (*P. fermentans*, *Geotrichum candidum*, and *P. kudriavzevi*) decreased from the S- to the C-layer. These microbes are usually unable to tolerate high temperature. The RAs of the thermotolerant bacterial species *B. licheniformis* and fungal species *T. aurantiacus* increased from the S- to the C-layer. These biomarkers have often been found in different types of conventional food starter, such as MT-Daqu, LT-Daqu, and Xiaoqu (Xu et al., 2022). In the early fermentation stage, due to the different RA of LABs in different parts of Daqu, the pH and total acidity of different parts were different. Specifically, most LAB was significantly correlated with lactic acid, acetic acid, pH and acidity at different parts of Daqu during the fermentation (Figs. S5a, 5c, and 5e). During the Daqu fermentation process, *B. licheniformis* and *L. ramosa* exhibited a strong positive correlation ($p < 0.01$) with the saccharifying and liquifying activities mainly in the S-layer (Fig. S5), which likely contributes to the

notably higher saccharifying and liquifying activities observed in the S-layer compared to other parts.

3.3. Co-occurrence patterns of microbial community and keystone taxa

The co-occurrence patterns in the microbial communities of different parts of Daqu were analyzed to elucidate potential interactions among the microorganisms within the microbial communities. As shown in Fig. 4a–c, positive correlations emerged as the prevailing interactions across all co-occurrence networks, suggesting potential coexistence of the microbes in the forms of commensalism, cooperation, mutualism, or syntrophy, thereby contributing to the stability of the microbial community structure (Li et al., 2024). Notably, the percentage of negative interaction was higher in the S-layer (33.88%) than in the M-layer (28.76%) and the C-layer (33.01%) (Fig. 4a–c), reflecting possibly more intense competition for limited resources or unique environmental niches generated by microbial metabolism in the S-layer (Zhang et al., 2022a). Bacillota were the most abundant bacterial taxon in all networks, collectively accounting for 35.42%, 37.04%, and 36.84% of the total nodes in the S-, M-, and C-layer, respectively; while Ascomycota was the most abundant fungal taxon in all networks, accounting for 45.83%, 48.15%, and 45.61% of the total nodes in the S-, M-, and C-layer, respectively (Fig. 4a–c). This analysis indicated that Bacillota and Ascomycota were not only the most abundant phyla but also widely distributed across all networks, potentially contributing to the enhanced tightness and stability of the overall network structure (Tang et al., 2023).

The topological characteristics were utilized to depict the intricate pattern of interdependence among dominant microorganisms (Table 1). The M- and C-layer exhibited a higher clustering coefficient and degree centralization, and a lower average path length, indicating closer interrelationships among these microbes in these layers than in the S-layer. Specifically, the S-layer contained 48 nodes connected by 183 edges, the M-layer had 54 nodes connected by 233 edges, and the C-

Table 1
Differences in the topology properties of molecular ecological network.

Network Properties [a]	S-layer	M-layer	C-layer
Average degree	7.625	8.630	7.333
Average path length	2.504	1.705	2.374
Network diameter	3.339	5.330	7.356
Network density	0.162	0.163	0.131
Clustering coefficient	0.507	0.538	0.624
Centralization betweenness	0.197	0.157	0.268
Degree centralization	0.221	0.253	0.244
Modularity	0.468	0.292	0.344
Degree kurtosis	2.362	1.972	2.175
Degree skewness	0.475	0.536	0.664

[a] All properties were obtained from the molecular ecological network analysis pipeline.

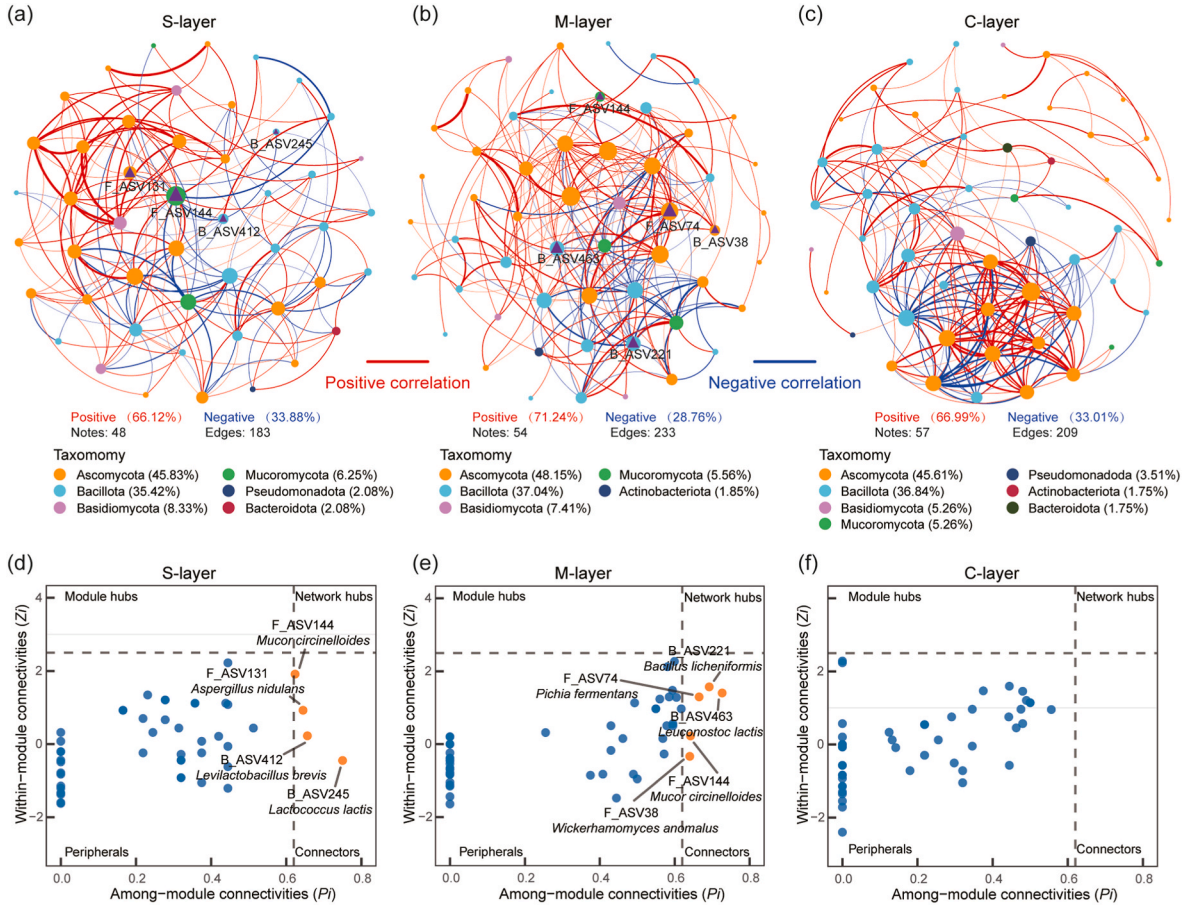

Fig. 4. The co-occurrence network diagrams (a–c) and keystone taxa (d–f) in different parts of MT-Daqu during fermentation. Each node represents a ASV and the size of the node is proportional to the degree of the ASV. The linkages (edges) indicate significant co-occurrence relationships with a significant correlation ($p < 0.05$); red and blue lines indicate positive and negative relationships, respectively. The purple triangles within the nodes represented keystone taxa in the co-occurrence network in different parts of MT-Daqu. Keystone taxa are identified based on the node topological properties in each network, with thresholds of intra-module connectivity (Zi) > 2.5 and/or inter-module connectivity (Pi) > 0.62. ASVs were selected with relative abundance ≥0.01% and occurred in more than 1/5 of the total sample size in order to construct a symbiotic network of microbial communities using Spearman's correlation ($|r| > 0.6$, $p < 0.05$). (For interpretation of the references to color in this figure legend, the reader is referred to the Web version of this article.)

layer consisted of 57 nodes linked by 209 edges (Fig. 4a–c), suggesting that the microbial co-occurrence network complexity was lower in the S-layer compared to the M-layer and C-layer. A study demonstrated that weak interactions could result in more stable temporal ecological networks (Coyte et al., 2015). Thus, the microbial network with greater stability in the S-layer might better withstand significant changes in the external environment, particularly at the solid-gas interface, and assist in minimizing the adverse impacts of environmental microorganisms on Daqu fermentation.

The positioning of a node (ASV) in the network is defined by the 'within-module connectivity' (Zi) and 'among-module connectivity' (Pi). Typically, network hubs, module hubs, and connectors are recognized as harboring crucial species that facilitate community formation and potentially influence community structure maintenance. Removal of these taxa may lead to the disintegration of modules and networks (Yuan et al., 2021). Based on the connectivity (Zi < 2.5, Pi > 0.62), four, five and zero ASVs were identified as keystone taxa from the S-, M- and C-layer, respectively (Fig. 4d–f). The keystone taxa of the S-layer were *Mucor circinelloides*, *Aspergillus nidulans*, *Levilactobacillus brevis*, and *Lactococcus lactis*; while the keystone taxa of the M-layer included *B. licheniformis*, *P. fermentans*, *L. lactis*, *M. circinelloides*, and *W. anomalus*. The number of keystone taxa typically correlate with the size and complexity of the network, and the absence of such taxa can result in network fragmentation and functional alterations (Mu et al., 2023). Additionally, these keystone taxa can influence microbial community structure and assembly via diverse mechanisms, including secreting extracellular enzymes that hydrolyze polysaccharides to generate nutrients utilized by other microorganisms for growth and reproduction, and excreting microbial growth inhibitors to restrain the proliferation of other species. For example, in addition to its ability to produce amylase and/or protease, *B. licheniformis, P. fermentans,* and *L. lactis* also exhibit antagonistic properties, which can effectively inhibit the growth of various harmful bacteria and microorganisms (Lawrance et al., 2014; Pal and Sharma, 2019; Zong et al., 2024), so as to ensure the normal fermentation of Daqu. Therefore, these keystone taxa, primarily located outside the C-layer, can help the microbial network effectively resist the interference of environmental microorganisms, and play an important role in driving community assembly, maintaining niche stability, and

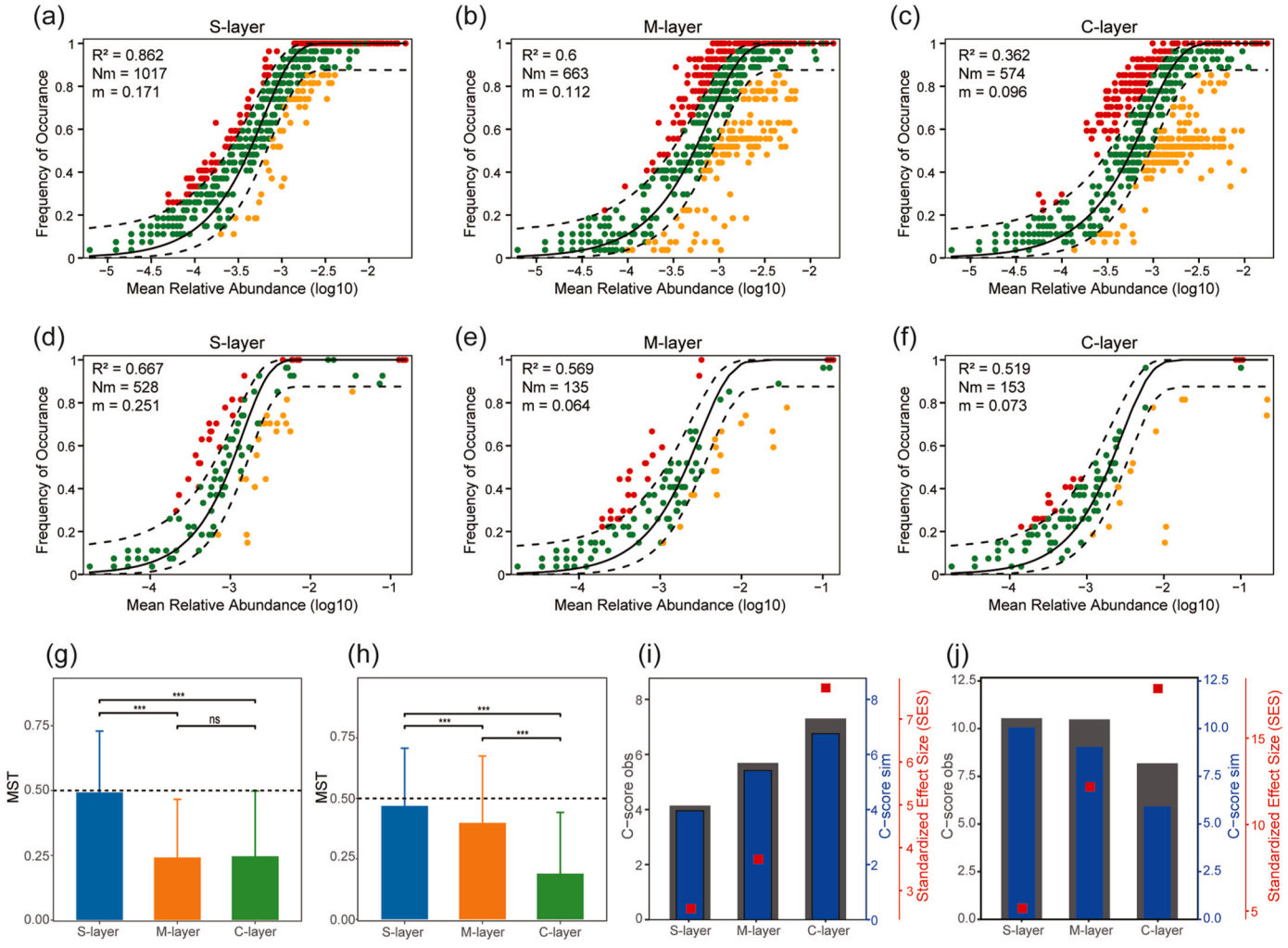

Fig. 5. Ecological processes of microbial community assemblies in different parts of MT-Daqu. The predicted occurrence frequencies of bacterial (a–c) and fungal (d–f) communities in different parts of MT-Daqu. The red and orange circles represent ASVs that occurred more and less frequently than predicted, respectively. The solid black line indicates the best fit to the neutral community model (NCM), and the dashed black line indicates 95% confidence intervals. m is the estimated migration rate, Nm is the product of metacommunity size and m values, and R^2 represents the fit to the neutral community model. Modified normalized stochasticity ratios (MST) were estimated to measure the relative importance of deterministic processes of bacterial (g) and fungal (h) community assemblies based on Jaccard distance. The horizontal dashed black line (MST = 0.5) was set as the boundary between deterministic (MST <0.5) and stochastic (MST >0.5) assembly processes. The C-score metric was used with null models for bacterial (i) and fungal (j) communities. Values of the observed C-score (C-score obs) > simulated C-score (C-score sim) indicate non-random co-occurrence patterns. Standardized effect size < −2 and >2 represent aggregation and segregation, respectively. ***, $p < 0.001$; **, $p < 0.01$; *, $p < 0.05$; ns, not significant. (For interpretation of the references to color in this figure legend, the reader is referred to the Web version of this article.)

performing metabolic functions.

3.4. Assembly processes of the microbial communities in different parts of Daqu

Understanding the assembly process of microbial communities is crucial for the targeted regulation of functional species (Huang et al., 2023). Multiple models were adopted to investigate the causes of the differences in the assembly patterns of the microbial communities in different parts of Daqu during fermentation. The relationship between the occurrence frequency of ASVs and their relative abundance was analyzed using the Neutral Community Model (NCM) (Fig. 5a–f). The relative contribution of stochastic processes gradually decreased from the S- to the C-layer in both the bacterial and fungal communities, with 86.2%, 60.0%, and 36.2% of explained community variance (R^2 values) for the bacterial community of the S-, M-, and C-layer, respectively; and 66.7%, 56.9%, and 51.9% for the fungal community of the corresponding parts. The result indicated that the NCM fitted well for the bacterial and fungal communities in different parts of Daqu with a moderate fitted value. The migration rate (m) estimated by the neutral model reflects the dispersal ability of the species (Yang et al., 2023). The migration rates were low and gradually decreased in both the bacterial and fungal communities from the S- to the C-layer, with rates of 0.171 for bacteria and 0.251 for fungi in the S-layer; 0.112 for bacteria and 0.064 for fungi in the M-layer; and 0.096 for bacteria and 0.073 for fungi in the C-layer (Fig. 5a–f). These patterns indicated that stochastic processes contribute less and less to both bacterial and fungal community construction from the S- to the C-layer, with deterministic processes dominating the overall community structures.

The community-level niche breadths were estimated to reveal the contributions of deterministic and stochastic processes to microbial community assembly. Our results indicated that, from the S- to C-layer, niche breadth of microbial community showed a significant trend of decrease ($R^2 = 0.19$, $p < 0.05$ for bacteria and $R^2 = 0.46$, $p < 0.001$ for fungi) (Fig. S6), implying that the community assembly was more strongly influenced by deterministic processes in the C-layer. At the community level, a microbial community with a broad niche breadth indicates a more degree of competitiveness, adaptability and stability than the one with a narrow niche breadth (Pandit et al., 2009). The microbial community of the S-layer exhibited a wider niche breadth compared to those of the other parts (Fig. S6), indicating that it can adapt to a broader range of habitat niches than the microbial communities of the other parts, thereby displaying strong resistance; whereas the microbial communities of the other parts were more susceptible to disturbances. The result was consistent with the analysis of topological properties in the co-correlation networks (Fig. 4a–c and Table 1).

To further quantify the relative importance of stochastic and deterministic processes in shaping the bacterial and fungal communities in the different parts of Daqu, we calculated the modified normalized stochasticity ratio (MST) in each layer (Fig. 5g–h). This framework was developed with 0.5 as the boundary point between more stochastic (MST >0.5) and deterministic (MST <0.5) assembly processes. The average MST value of the microbial community in all parts was less than 0.5, indicating that deterministic processes dominated the community assembly. Notably, from the S- to the C-layer, the MST values decreased significantly ($p < 0.001$), also indicating a gradual enhancement of the deterministic processes in the microbial community. The conclusion was further supported by the C-score results, which showed that the value of the standardized effect size (SES) gradually increased from the S- to the C-layer (Fig. 5i–j), indicating the enhanced importance of deterministic processes in the assembly of the bacterial and fungal communities.

Our results obtained from multiple models suggest that deterministic processes played a dominant role in the formation of bacterial and fungal communities in different parts of Daqu during fermentation, and the impact of deterministic processes on microbial community assembly progressively increased from the S- to the C-layer. This phenomenon can be attributed to several factors. Firstly, the S-layer, being in direct contact with the surrounding environment during fermentation, experiences a higher influx of environmental microorganisms, leading to increased immigration rates and greater microbial diversity, thereby decreasing the deterministic processes within the S-layer microbial communities. On the other hand, the microorganisms in the S-layer may encounter lower physiological stress levels (such as temperature, CO_2 and O_2 level), enabling them to proliferate more freely and thereby reducing the impact of deterministic processes. Our results are not in agreement with previous findings in HT-Daqu, which noted that stochastic processes governed the fungal community assembly, whereas deterministic assembly processes dominated the bacterial community in HT-Daqu (Huang et al., 2024; Shi et al., 2024). The variation in production processes may account for these differences. HT-Daqu, which is characterized by higher fermentation temperatures and longer fermentation durations, differs from MT-Daqu. The bacterial community plays a crucial role in the functionality of HT-Daqu, hence it is commonly known as bacterial Daqu.

3.5. Potential driving factors of microbial community succession and assembly

To investigate the potential driving factors of the differences in microbial community compositions in different parts of Daqu during fermentation, the relative abundance of the 19 biomarkers predicted was assessed by random forest analysis (Fig. S4). Most endogenous factors were significantly correlated with bacterial biomarkers (such as *W. confusa*, *B. licheniformis*, and *P. pentosaceus*) and fungal biomarkers (such as *P. fermentans*, *G. candidum*, and *L. ramosa*) in different parts of Daqu (Fig. S5), implying that these factors may cause the differences in microbial diversity and community composition in different parts of Daqu. Meanwhile, most endogenous factors were found to exert a unique influence on each biomarker in different parts of Daqu, and they may therefore drive the shape of different microbial community assembly models during Daqu fermentation through distinct mechanisms (Ma et al., 2022).

To further investigate the endogenous factors influencing microbial community assembly in different parts of Daqu during fermentation, we conducted Mantel tests to assess the correlation between microbial composition and each endogenous factor (Fig. 6a–b). Various endogenous factors exerted different degrees of influence on the microbial community composition in different parts of Daqu during the fermentation process, with a primary positive correlation. Compared with the M- and C-layers, more endogenous factors were significantly correlated with the bacterial and fungal communities in the S-layer. Meanwhile, the influence of endogenous factors on the fungal community was more pronounced. Moisture, maltose, fructose, ethanol, succinic acid, lactic acid, acetic acid, and total amino acid were the strongest correlates ($r > 0.4$, $p < 0.01$) of the fungal and bacterial communities in different parts of Daqu. Notably, the same endogenous factor has different degree of correlation with the bacterial and fungal communities in different parts of Daqu. Temperature had the strongest correlation with the bacterial community in the S-layer ($r = 0.41$, $p < 0.01$), followed by the M- ($r = 0.23$, $p < 0.01$) and C-layer ($r = 0.17$, $p < 0.01$), while temperature had the strongest correlation with the fungal community in the C-layer ($r = 0.30$, $p < 0.01$), followed by the M- ($r = 0.22$, $p < 0.01$) and the S-layer ($r = 0.19$, $p < 0.05$). The above results indicated that these endogenous factors, as abiotic selection pressures, have potential effects on the microbial community succession during fermentation (Li et al., 2024).

The major potential driving factors of microbial community assembly during Daqu fermentation were further determined by random forest algorithm analysis (Fig. 6c and d). Temperature ($p < 0.01$), acetic acid ($p < 0.01$), maltose ($p < 0.05$), and ethanol ($p < 0.05$) were found to be significant factors in explaining bacterial community assembly (Fig. 6c), while temperature ($p < 0.01$) was significant factors in explaining fungal community assembly (Fig. 6d). The findings suggest that these

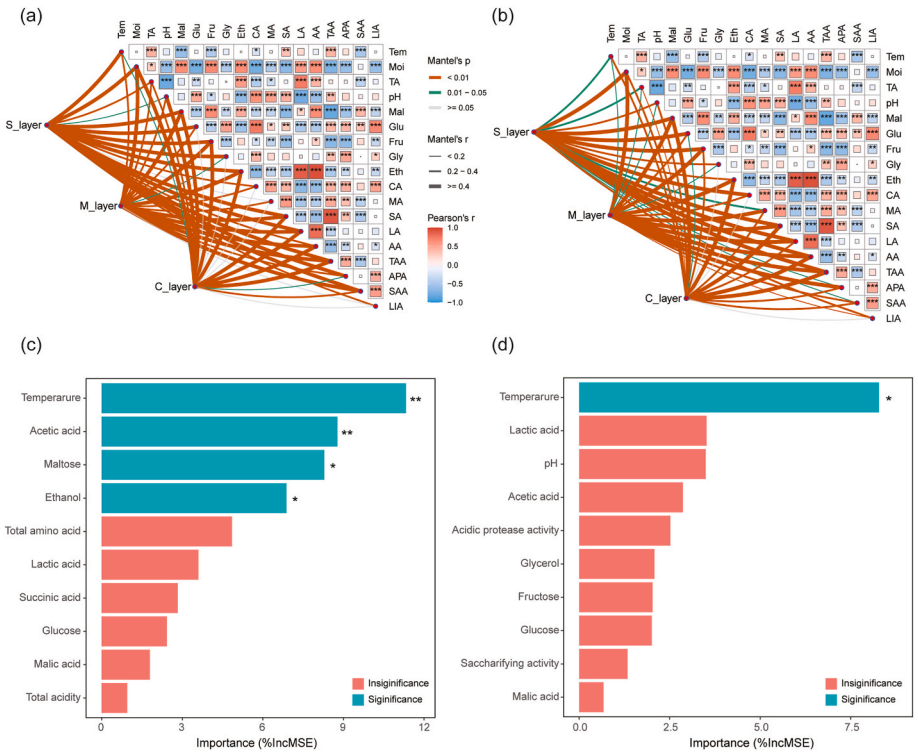

Fig. 6. Effects of endogenous factors on the microbial community composition in different parts of MT-Daqu and potential driving factors of microbial community assembly. Pairwise comparisons of endogenous factors are shown at the upper-right, with a color gradient representing Pearson's correlation coefficients. The Mantel test analyzed the relationship between endogenous factors and the bacterial (a) and fungal (b) community compositions. The thickness of the lines represents the Mantel's r statistic for the corresponding correlation and line colors mean significance. The random forest learning algorithm predicted the importance of endogenous factors as drivers of the assembly of bacterial (c) and fungal (d) communities. The percentage increase in mean square error (%IncMSE) of the variables was used to estimate the importance of these predictors, where higher values of %IncMSE indicate more important predictors. **, $p < 0.01$; *, $p < 0.05$. (For interpretation of the references to color in this figure legend, the reader is referred to the Web version of this article.)

endogenous factors may directly influence the assembly of microbial communities in different parts of Daqu. Temperature is a crucial fermentation parameter that directly influences microbial metabolism and growth. Prior studies have shown that the fermentation peak-temperature is a pivotal factor on deterministic assembly in communities in Daqu fermentation (Huang et al., 2024), and differences in temperature could increase the proportion of deterministic processes (He et al., 2021). Acetic acid affects the structure and metabolism of bacterial cells, inhibiting the growth of numerous spoilage bacteria (Zheng et al., 2013), and thereby regulating bacterial community assembly. The assembly processes of bacterial and fungal communities in different parts of Daqu were affected by various endogenous factors, with fermentation temperature being the most crucial driving force for the assembly of these communities. Additionally, the main microbial taxa and co-occurrence network patterns in different parts of Daqu also showed significant differences. Therefore, the deterministic processes of bacterial and fungal communities in different parts of Daqu were mainly controlled by deterministic factors (abiotic environmental conditions and species interaction) (Shi et al., 2024; Yang et al., 2023), which fit ecological niche theory.

The above research will help us to understand the reasons for the differentiation of microbial communities in different parts of Daqu, which is crucial for the targeted regulation of functional species of Daqu to improve the quality of Daqu. At the initial stage (Phase I) of Daqu fermentation with high water content, favorable nutritional and environmental conditions for the growth of facultative anaerobic microorganisms (such as LAB and yeasts) were provided, making these microorganisms the dominant microbiota in different parts of Daqu (Fig. 3c and h). Variations in reducing sugars could influence the composition of the microbial community, possibly stemming from differences in sugar preferences and metabolic pathways among various microorganisms (Wang et al., 2021). During the initial fermentation phase, the escalating production of ethanol by yeasts can suppress the growth of specific filamentous fungi and bacteria (Wu et al., 2021), thereby impacting the microbial community composition. The majority of organic acids (especially lactic acid and acetic acid) found in spontaneously fermented foods are generated through bacterial metabolism, playing a crucial role in regulating the microbial community and enhancing the quality and aroma of such products (Huang et al., 2022). The organic acids produced by the metabolism of microorganisms can increase the acidity and decrease the pH of the habitat, thus inhibiting the growth of acid-nonresistant microorganisms. Additionally, they can also serve as a prerequisite for the synthesis of various esters and other flavor substances. Furthermore, amino acids, as essential nutrients in the fermentation ecosystem following carbon compounds, play a crucial role in regulating the microbial community composition by influencing the growth and fermentation kinetics of microorganisms. Enzymes primarily influence microbial community structure through the decomposition of products derived from raw materials, as these products can provide abundant nutrients for microbial growth. Thus, these findings underscore the connection between endogenous factors and microbial community composition, which may further impact community assembly processes.

4. Conclusion

This study showed that the microbial communities were obviously different in different parts of Daqu during fermentation. The microbial communities began to differentiate from the initial fermentation stage, resulting in the differences in the main microbial taxa and co-occurrence

network patterns in different parts. Multiple community assembly models confirmed that deterministic processes dominated the community assembly in different parts, gradually increasing from the surface to the core layer. The main endogenous driving factors of bacterial community assembly differed from those of fungal community assembly. These results provide new insights into the understanding of microbial community assembly in Daqu and are valuable for the quality control of Daqu production.

CRediT authorship contribution statement

Zhang Wen: Methodology, Investigation, Conceptualization, Data curation, Visualization, Writing – original draft. **Pei-Jie Han:** Resources, Supervision, Funding acquisition, Project administration, Writing – review & editing. **Da-Yong Han:** Methodology, Formal analysis, Funding acquisition. **Liang Song:** Methodology, Funding acquisition. **Yu-Hua Wei:** Investigation, Methodology. **Hai-Yan Zhu:** Supervision, Conceptualization. **Jie Chen:** Investigation. **Zheng-Xiang Guo:** Investigation. **Feng-Yan Bai:** Conceptualization, Resources, Supervision, Writing – review & editing.

Declaration of competing interest

The authors declare that they have no known competing financial interests or personal relationships that could have appeared to influence the work reported in this paper.

Acknowledgements

This study was supported by the National Natural Science Foundation of China (No. 32170011), the Youth Innovation Promotion Association of the Chinese Academy of Sciences (No. 2022087), the Young Scientists Fund of the National Natural Science Foundation of China (No. 32200006), and the Young Scientists Fund of the National Natural Science Foundation of China (No. 32300007).

Appendix A. Supplementary data

Supplementary data to this article can be found online at https://doi.org/10.1016/j.crfs.2024.100883.

Data availability

Data will be made available on request.

References

Coyte, K.Z., Schluter, J., Foster, K.R., 2015. The ecology of the microbiome: networks, competition, and stability. Science 350 (6261), 663–666. https://doi.org/10.1126/science.aad2602.

Ding, L., Zhao, M., Zhao, X., Chen, G., Jiang, Q., Liu, M., Xiong, Y., Zhang, X., Wang, X., Wei, Y., Zheng, Y., Li, W., 2022. Evaluation of the spatial distribution and dynamic succession of microbial community and quality properties during fermentation in Chinese medium-temperature Daqu. J. Food Process. Preserv. 46 (12), e17272. https://doi.org/10.1111/jfpp.17272.

Du, H., Wei, J., Zhang, X., Xu, Y., 2022. Biocontrol of geosmin production by inoculation of native microbiota during the daqu-making process. Fermentation 8 (11), 588. https://doi.org/10.3390/fermentation8110588.

Han, P.-J., Song, L., Wen, Z., Zhu, H.-Y., Wei, Y.-H., Wang, J.-W., Bai, M., Luo, L.-J., Wang, J.-W., Chen, S.-X., You, X.-L., Han, D.-Y., Bai, F.-Y., 2024. Species-level understanding of the bacterial community in Daqu based on full-length 16S rRNA gene sequences. Food Microbiol. 123, 104566. https://doi.org/10.1016/j.fm.2024.104566.

Han, P., Luo, L., Han, Y., Song, L., Zhen, P., Han, D., Wei, Y., Zhou, X., Wen, Z., Qiu, J.-Z. J.F., 2023. Microbial community affects Daqu quality and the production of ethanol and flavor compounds in Baijiu fermentation. Foods 12 (15), 2936. https://doi.org/10.3390/foods12152936.

He, M., Jin, Y., Liu, M., Yang, G., Zhou, R., Zhao, J., Wu, C., 2023. Metaproteomic investigation of enzyme profile in daqu used for the production of Nongxiangxing baijiu. Int. J. Food Microbiol. 400, 110250. https://doi.org/10.1016/j.ijfoodmicro.2023.110250.

He, Q., Wang, S., Hou, W., Feng, K., Li, F., Hai, W., Zhang, Y., Sun, Y., Deng, Y., 2021. Temperature and microbial interactions drive the deterministic assembly processes in sediments of hot springs. Sci. Total Environ. 772, 145465. https://doi.org/10.1016/j.scitotenv.2021.145465.

Huang, P., Jin, Y., Liu, M., Peng, L., Yang, G., Luo, Z., Jiang, D., Zhao, J., Zhou, R., Wu, C., 2023. Exploring the successions in microbial community and flavor of daqu during fermentation produced by different pressing patterns. Foods 12 (13), 2603. https://doi.org/10.3390/foods12132603.

Huang, T., Lu, Z., Peng, M., Liu, Z., Chai, L., Zhang, X., Shi, J., Li, Q., Xu, Z., 2022. Combined effects of fermentation starters and environmental factors on the microbial community assembly and flavor formation of Zhenjiang aromatic vinegar. Food Res. Int. 152, 110900. https://doi.org/10.1016/j.foodres.2021.110900.

Huang, Y., Li, D., Mu, Y., Zhu, Z., Wu, Y., Qi, Q., Mu, Y., Su, W., 2024. Exploring the heterogeneity of community and function and correspondence of "species-enzymes" among three types of Daqu with different fermentation peak-temperature via high-throughput sequencing and metagenomics. Food Res. Int. 176, 113805. https://doi.org/10.1016/j.foodres.2023.113805.

Jin, G., Zhu, Y., Xu, Y., 2017. Mystery behind Chinese liquor fermentation. Trends Food Sci. Technol. 63, 18–28. https://doi.org/10.1016/j.tifs.2017.02.016.

Karst, S.M., Ziels, R.M., Kirkegaard, R.H., Sørensen, E.A., McDonald, D., Zhu, Q., Knight, R., Albertsen, M., 2021. High-accuracy long-read amplicon sequences using unique molecular identifiers with Nanopore or PacBio sequencing. Nat. Methods 18 (2), 165–169. https://doi.org/10.1038/s41592-020-01041-y.

Lawrance, A., Balakrishnan, M., Joseph, T.C., Palaiya Sukumaran, D., Nambali Valsalan, V., Gopal, D., Ramalingam, K., 2014. Functional and molecular characterization of a lipopeptide surfactant from the marine sponge-associated eubacteria Bacillus licheniformis NIOT-AMKV06 of Andaman and Nicobar Islands, India. Mar. Pollut. Bull. 82 (1), 76–85. https://doi.org/10.1016/j.marpolbul.2014.03.018.

Li, M., Lao, F., Pan, X., Yuan, L., Zhang, D., Wu, J., 2024. Insights into the mechanisms driving microbial community succession during pepper fermentation: roles of microbial interactions and endogenous environmental changes. Food Res. Int. 179, 114033. https://doi.org/10.1016/j.foodres.2024.114033.

Li, P., Lin, W., Liu, X., Wang, X., Luo, L., 2016. Environmental factors affecting microbiota dynamics during traditional solid-state fermentation of Chinese daqu starter. Front. Microbiol. 7 (1237). https://doi.org/10.3389/fmicb.2016.01237.

Li, Z., Fernandez, K.X., Vederas, J.C., Gänzle, M.G., 2023. Composition and activity of antifungal lipopeptides produced by Bacillus spp. in daqu fermentation. Food Microbiol. 111, 104211. https://doi.org/10.1016/j.fm.2022.104211.

Luo, L.J., Song, L., Han, Y., Zhen, P., Han, D.Y., Zhao, X., Zhou, X., Wei, Y.H., Yu, H.X., Han, P.J., Bai, F.Y., 2023. Microbial communities and their correlation with flavor compound formation during the mechanized production of light-flavor Baijiu. Food Res. Int. 113139. https://doi.org/10.1016/j.foodres.2023.113139.

Ma, S., Luo, H., Zhao, D., Qiao, Z., Zheng, J., An, M., Huang, D., 2022. Environmental factors and interactions among microorganisms drive microbial community succession during fermentation of Nongxiangxing daqu. Bioresour. Technol. 345, 126549. https://doi.org/10.1016/j.biortech.2021.126549.

Mo, Y., Peng, F., Gao, X., Xiao, P., Logares, R., Jeppesen, E., Ren, K., Xue, Y., Yang, J., 2021. Low shifts in salinity determined assembly processes and network stability of microeukaryotic plankton communities in a subtropical urban reservoir. Microbiome 9 (1), 128. https://doi.org/10.1186/s40168-021-01079-w.

Mu, Y., Huang, J., Zhou, R., Zhang, S., Qin, H., Tang, H., Pan, Q., Tang, H., 2023. Bioaugmented Daqu-induced variation in community succession rate strengthens the interaction and metabolic function of microbiota during strong-flavor Baijiu fermentation. LWT 182, 114806. https://doi.org/10.1016/j.lwt.2023.114806.

Nemergut, D.R., Schmidt, S.K., Fukami, T., O'Neill, S.P., Bilinski, T.M., Stanish, L.F., Knelman, J.E., Darcy, J.L., Lynch, R.C., Wickey, P., 2013. Patterns and processes of microbial community assembly. Microbiol. Mol. Biol. Rev. 77 (3), 342–356. https://doi.org/10.1128/mmbr.00051-12.

Nilsson, R.H., Tedersoo, L., Ryberg, M., Kristiansson, E., Hartmann, M., Unterseher, M., Porter, T.M., Bengtsson-Palme, J., Walker, D.M., De Sousa, F., 2015. A comprehensive, automatically updated fungal ITS sequence dataset for reference-based chimera control in environmental sequencing efforts. Microb. Environ. 30 (2), 145–150. https://doi.org/10.1264/jsme2.ME14121.

Ning, D., Deng, Y., Tiedje, J.M., Zhou, J., 2019. A general framework for quantitatively assessing ecological stochasticity. Proc. Natl. Acad. Sci. USA 116 (34), 16892–16898. https://doi.org/10.1073/pnas.1904623116.

Pal, M., Sharma, R.K., 2019. Exoelectrogenic response of Pichia fermentans influenced by mediator and reactor design. J. Biosci. Bioeng. 127 (6), 714–720. https://doi.org/10.1016/j.jbiosc.2018.11.004.

Pan, F., Qiu, S., Lv, Y., Li, D., 2023. Exploring the controllability of the Baijiu fermentation process with microbiota orientation. Food Res. Int. 173, 113249. https://doi.org/10.1016/j.foodres.2023.113249.

Pandit, S.N., Kolasa, J., Cottenie, K., 2009. Contrasts between habitat generalists and specialists: an empirical extension to the basic metacommunity framework. Ecology 90 (8), 2253–2262. https://doi.org/10.1890/08-0851.1.

Parry, N.J., Beever, D.E., Owen, E., Vandenberghe, I., Beeumen, J.V.A.N., Bhat, M.K., 2000. Biochemical characterization and mechanism of action of a thermostable β-glucosidase purified from Thermoascus aurantiacus. Biochem. J. 353 (1), 117–127. https://doi.org/10.1042/bj3530117.

Prodan, A., Tremaroli, V., Brolin, H., Zwinderman, A.H., Nieuwdorp, M., Levin, E., 2020. Comparing bioinformatic pipelines for microbial 16S rRNA amplicon sequencing. PLoS One 15 (1), e0227434. https://doi.org/10.1371/journal.pone.0227434.

Rognes, T., Flouri, T., Nichols, B., Quince, C., Mahé, F., 2016. VSEARCH: a versatile open source tool for metagenomics. PeerJ 4, e2584. https://doi.org/10.7717/peerj.2584.

Sakandar, H.A., Hussain, R., Farid Khan, Q., Zhang, H., 2020. Functional microbiota in Chinese traditional Baijiu and Mijiu Qu (starters): a review. Food Res. Int. 138, 109830. https://doi.org/10.1016/j.foodres.2020.109830.

Shanqimuge, Liang, H., Zhang, C., Shao, C., Peng, X., Liang, L., Su, J., Li, C., 2015. A DGGE marker-mediated fast monitoring of bacterial diversity and comprehensive identification of high-temperature daqu starter. J. Food Sci. 80 (7), M1519–M1525. https://doi.org/10.1111/1750-3841.12903.

Shi, G., Fang, C., Xing, S., Guo, Y., Li, X., Han, X., Lin, L., Zhang, C., 2024. Heterogenetic mechanism in high-temperature Daqu fermentation by traditional craft and mechanical craft: from microbial assembly patterns to metabolism phenotypes. Food Res. Int. 187, 114327. https://doi.org/10.1016/j.foodres.2024.114327.

Tang, J., Rao, J., Zou, Y., Liao, L., Huang, D., Luo, H., 2023. The community assembly patterns determined differences between the surface and the core microbial communities of Nongxiangxing Daqu. LWT 183, 114936. https://doi.org/10.1016/j.lwt.2023.114936.

Wang, Z., Ji, X., Wang, S., Wu, Q., Xu, Y., 2021. Sugar profile regulates the microbial metabolic diversity in Chinese Baijiu fermentation. Int. J. Food Microbiol. 359, 109426. https://doi.org/10.1016/j.ijfoodmicro.2021.109426.

Wu, Q., Zhu, Y., Fang, C., Wijffels, R.H., Xu, Y., 2021. Can we control microbiota in spontaneous food fermentation? – Chinese liquor as a case example. Trends Food Sci. Technol. 110, 321–331. https://doi.org/10.1016/j.tifs.2021.02.011.

Wu, S., Du, H., Xu, Y., 2023. Daqu microbiota adaptability to altered temperature determines the formation of characteristic compounds. Int. J. Food Microbiol. 385, 109995. https://doi.org/10.1016/j.ijfoodmicro.2022.109995.

Xia, Y., Luo, H., Wu, Z., Zhang, W., 2023. Microbial diversity in jiuqu and its fermentation features: saccharification, alcohol fermentation and flavors generation. Appl. Microbiol. Biotechnol. 107 (1), 25–41. https://doi.org/10.1007/s00253-022-12291-5.

Xiao, C., Lu, Z., Zhang, X., Wang, S., Ao, L., Shen, C., Shi, J., Xu, Z., Björkroth, J., 2017. Bio-heat is a key environmental driver shaping the microbial community of medium-temperature daqu. Appl. Environ. Microbiol. 83 (23), e01550. https://doi.org/10.1128/AEM.01550-17, 17.

Xu, Y., Zhao, J., Liu, X., Zhang, C., Zhao, Z., Li, X., Sun, B., 2022. Flavor mystery of Chinese traditional fermented baijiu: the great contribution of ester compounds. Food Chem. 369, 130920. https://doi.org/10.1016/j.foodchem.2021.130920.

Yang, H., Peng, Q., Zhang, H., Sun, J., Shen, C., Han, X., 2022. The volatile profiles and microbiota structures of the wheat Qus used as traditional fermentation starters of Chinese rice wine from Shaoxing region. LWT 154, 112649. https://doi.org/10.1016/j.lwt.2021.112649.

Yang, Q., Zhang, P., Li, X., Yang, S., Chao, X., Liu, H., Ba, S., 2023. Distribution patterns and community assembly processes of eukaryotic microorganisms along an altitudinal gradient in the middle reaches of the Yarlung Zangbo River. Water Res. 239, 120047. https://doi.org/10.1016/j.watres.2023.120047.

Yang, S.-B., Fu, J.-J., He, J.-H., Zhang, X.-J., Chai, L.-J., Shi, J.-S., Wang, S.-T., Zhang, S.-Y., Shen, C.-H., Lu, Z.-M., Xu, Z.-H., 2024. Decoding the Qu-aroma of medium-temperature Daqu starter by volatilomics, aroma recombination, omission studies and sensory analysis. Food Chem. 457, 140186. https://doi.org/10.1016/j.foodchem.2024.140186.

Yuan, M.M., Guo, X., Wu, L., Zhang, Y., Xiao, N., Ning, D., Shi, Z., Zhou, X., Wu, L., Yang, Y., Tiedje, J.M., Zhou, J., 2021. Climate warming enhances microbial network complexity and stability. Nat. Clim. Change 11 (4), 343–348. https://doi.org/10.1038/s41558-021-00989-9.

Zhang, H., Tan, Y., Wei, J., Du, H., Xu, Y., 2022a. Fungal interactions strengthen the diversity-functioning relationship of solid-state fermentation systems. mSystems 7 (4), e00401. https://doi.org/10.1128/msystems.00401-22, 22.

Zhang, Y., Xu, J., Ding, F., Deng, W., Wang, X., Xue, Y., Chen, X., Han, B.Z., 2022b. Multidimensional profiling indicates the shifts and functionality of wheat-origin microbiota during high-temperature Daqu incubation. Food Res. Int. 156, 111191. https://doi.org/10.1016/j.foodres.2022.111191.

Zheng, L., Bae, Y., Jung, K., Heu, S., Lee, S., 2013. Antimicrobial activity of natural antimicrobial substances against spoilage bacteria isolated from fresh produce. Food Control 32 (2), 665–672. https://doi.org/10.1016/j.foodcont.2013.01.009.

Zong, E., Bo, T., Dang, L., Zhang, J., Li, H., Lv, N., He, Y., Bai, B., Zhang, J., Fan, S., 2024. Different functions can be provided by low temperature Daqu with different appearance features due to variations in the microbial community structure during fermentation. LWT 193, 115763. https://doi.org/10.1016/j.lwt.2024.115763.